

See discussions, stats, and author profiles for this publication at: <https://www.researchgate.net/publication/248899645>

Embryology of the dioecious Australian endemic *Lomandra longifolia* (Lomandraceae)

Article in *Australian Journal of Botany* · January 2008

DOI: 10.1071/BT07222

CITATIONS

6

READS

1,564

3 authors, including:



Nabil Ahmad

The University of Sydney

31 PUBLICATIONS 355 CITATIONS

SEE PROFILE

Embryology of the dioecious Australian endemic *Lomandra longifolia* (Lomandraceae)

Nabil M. Ahmad^A, Peter M. Martin^{A,B} and John M. Vella^A

^AAmenity Horticulture Unit, University of Sydney Plant Breeding Institute, PMB 11, Camden, NSW 2570, Australia.

^BCorresponding author. Email: pmartin@camden.usyd.edu.au

Abstract. Microsporogenesis, embryogeny and endosperm development of *Lomandra longifolia* Labill. are described in detail. The formation of the anther wall is the basic type composed of four cell layers, namely an epidermis, an endothecium, one middle layer and a tapetum. The tapetum layer has glandular, uninucleate cells. Successive cytokinesis follows meiosis, subsequently forming a tetrahedral tetrad of microspores. The ovule in each carpel is hemitropous, crassinucellate and bitegmic, with the micropyle formed by the inner integument. The archesporial cell divides periclinally to form the primary parietal and primary sporogenous cells. The sporogenous cell functions as the megaspore mother cell, whereas the parietal cell divides to give rise to two parietal layers. The mature megagametophyte, which has enlarged synergids and antipodals, is of the *Polygonum* type, with the normal complement of seven cells and eight nuclei. Nucellar tissue in the mature ovule consists of enlarged dermal cells and irregular subdermal cells surrounding a central strand of markedly smaller cells. Endosperm development is of the nuclear type. Embryo development is of the Graminad type, characterised by oblique zygotic and early pro-embryonic divisions.

Introduction

Lomandra is a genus of 50 species native to Australia, of which two species extend to New Guinea and one of these to New Caledonia (Lee and Macfarlane 1986). *L. longifolia*, the subject of this paper, is one of the most widely distributed *Lomandra* species, with a range along the coast and tablelands from North Queensland to south-eastern South Australia and eastern and northern Tasmania (Lee and Macfarlane 1986).

The systematic position of this genus has long been problematic; it was placed in the family Juncaceae by Bentham (1878) and by Bentham and Hooker (1880), then in Liliaceae (Krause 1930), Xanthorrhoeaceae (Cronquist 1981), Dasypogonaceae (Dahlgren *et al.* 1985), Xanthorrhoeaceae (Bedford *et al.* 1986) and more recently Lomandraceae (Brummitt 1992; Rudall and Chase 1996) and Laxmanniaceae (APG 1998; APGII 2003). The Australian Plant Name Index (2008) currently places *Lomandra* in the family Lomandraceae. There is considerable activity concerning relationships within the Asparagales (Rudall 1994; Rudall and Chase 1996; APGII 2003), suggesting that there will be further changes in relation to the preferred family placement of the genus *Lomandra*.

Rudall (1994) examined the ovule, the mature embryo sac and some aspects of megagametophyte development in several genera grouped by Bedford *et al.* (1986) under Xanthorrhoeaceae. She noted in *Lomandra* markedly enlarged cells in the chalazal dermal layer of the nucellus, and very large ('giant') synergids and antipodals. On the basis of this work and other anatomical and molecular studies, Rudall and Chase (1996) concluded that there are several generic groupings in Xanthorrhoeaceae *sensu lato* deserving recognition at family level and proposed a recircumscription of the family Lomandraceae (as originally defined by Lotsy in 1911) to include *Lomandra*,

Acanthocarpus, *Chamaexeros*, *Romnaldia*, *Xerolirion* and certain Arthropodioid genera such as *Thysanotus* and *Cordylina*.

Davis (1966), summarising the account of Schnarf and Wunderlich (1939), described the embryo-sac development of *Lomandra rigida* as follows: 'the archesporial cell cuts off a primary parietal cell which gives rise to three parietal layers, and the apical cells of the nucellar epidermis divide periclinally to form a nucellar cap three cells in thickness. Cytokinesis in the megaspore mother cell accompanies meiosis and the chalazal megaspore of a linear tetrad develops into a *Polygonum* type embryo sac. The synergids are pyriform and exhibit the filiform apparatus, the polar nuclei fuse before fertilisation, and three large antipodal cells are formed'. The paper of Schnarf and Wunderlich (1939) contains what seems to be the only published account of the sequence of embryo-sac development in any species of *Lomandra*; no information has been found in the literature on embryo development, endosperm development or microsporogenesis in *Lomandra*.

In the present paper, we describe in detail the embryological characters and endosperm development of *L. longifolia* as well as the process of microsporogenesis. It is hoped that this data, together with similar information on other *Lomandra* species and related genera, will contribute to furthering understanding of relationships and phylogeny within the family Lomandraceae and to evaluating relationships with allied families.

Materials and methods

Source of material

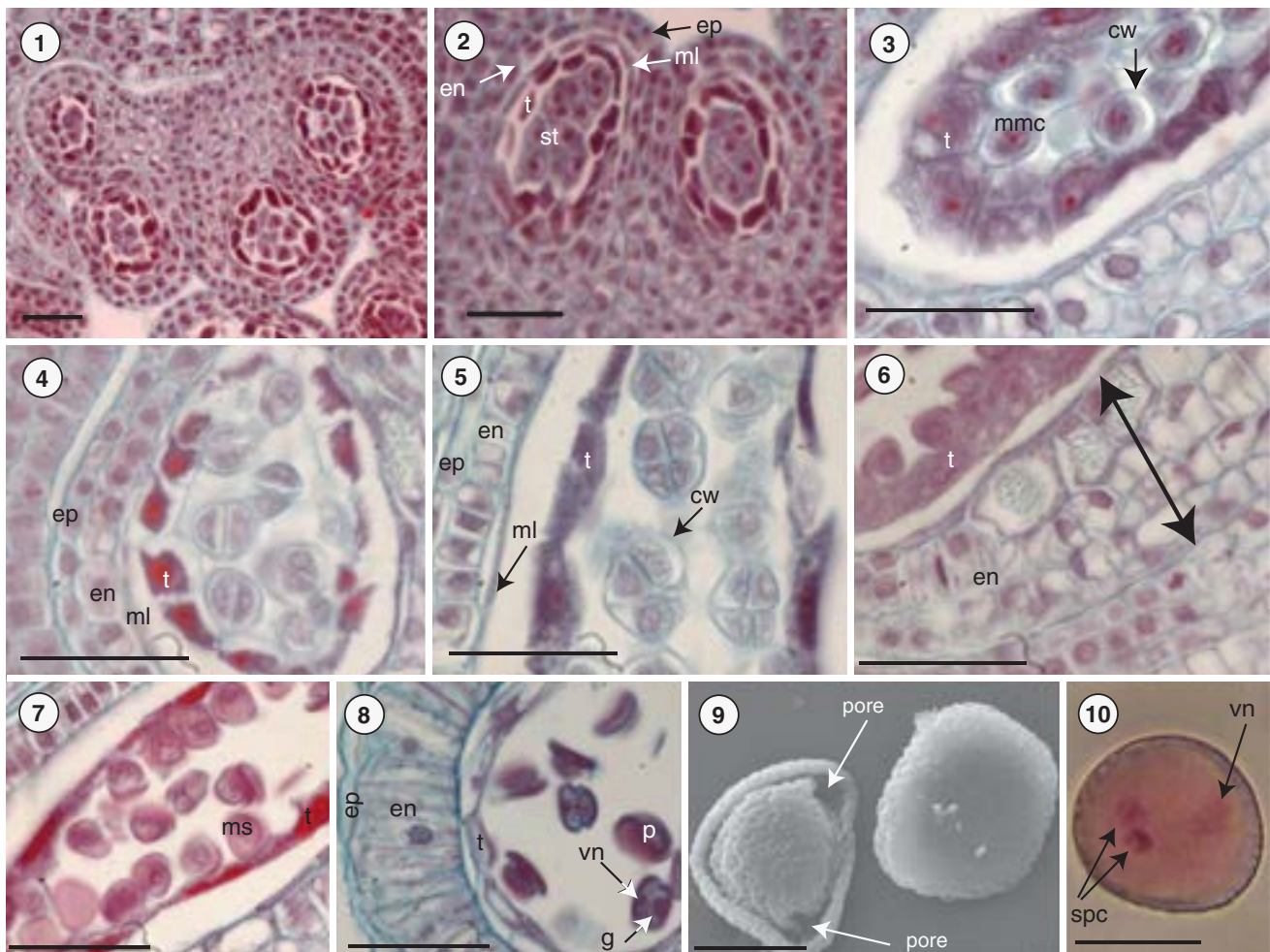
Plants of *L. longifolia* grown by Leppington Speedy[®] Seedlings Pty Ltd, Leppington, New South Wales, from seed collected in the Southern Highlands region of New South Wales, were supplied in nursery trays when ~5 cm high. These were grown to maturity and

maintained in the field at the Plant Breeding Institute at Cobbitty, New South Wales. Floral and fruit materials (buds, flowers, and fruits) of various developmental stages of *L. longifolia* were collected periodically from this plantation (every 2 days, from inflorescence emergence to seed ripening). Individual plants often had floral and fruit material at various stages of development, ranging from unopened buds through to immature fruits on different inflorescences. Vouchers of the male and female plants examined have been deposited in the Australian National Herbarium CANB (CANB 763117–CANB 763124).

For embryological studies, individual buds, flowers and seeds at different developmental stages were excised, dissected under a stereomicroscope and fixed in formalin acetic alcohol (FAA; 5 parts formalin : 5 parts glacial acetic acid : 90 parts 50% ethanol (v/v/v)) and stored in 70% ethanol. They were

dehydrated through an ethanol series and then embedded in paraffin with melting point 58–60°C for microtoming. Serial sections (longitudinal and transverse) cut with a rotary microtome (Spencer 820: American Optical Co, Buffalo, NY, USA) at 6–8 µm in thickness were stained with safranin-O and fast green FCF (Sass 1958), dehydrated through an alcohol series to 100% ethanol and mounted with DPX (BDH, Poole, UK). The samples were observed with normal brightfield optics on a Nikon Eclipse E800 light microscope (Nikon Optical Co, Tokyo, Japan) and photographed with a mounted Nikon Photo Head V-TP Sensicam camera (PCO CCD imaging: PCO Imaging, Kelheim, Germany).

For observations on food reserves in mature seeds, they were first softened by soaking in water and then sectioned by hand. Sections were tested immediately for the existence of oil droplets



Figs 1–10. Development of an anther and microspores in *Lomandra longifolia*. **Fig. 1.** Transverse section of a young anther showing two lobes and four microsporangia. **Fig. 2.** Four-cell-layered wall structure. **Fig. 3.** Isolation of individual microspore mother cells by callose wall. **Fig. 4.** Dyad formation. **Fig. 5.** Microsporangium showing the glandular tapetum and the tetrads in the callose wall. **Fig. 6.** Multilayered endothecium-like tissue. **Fig. 7.** Release of microspores by dissolution of callose wall. **Fig. 8.** Mature microsporangium with the middle layer degenerated and the cells of the endothecium enlarged and developing thickenings. **Fig. 9.** Scanning electron micrograph showing mature pollen grains in face and rear view. **Fig. 10.** Mature pollen grain with two sperm cells embedded in vegetative cell (nucleus on the right side). cw, callose wall; en, endothecium; ep, epidermis; g, generative cell; ml, middle layer; mmc, microspore mother cell; ms, microspore; p, pollen; spc, sperm cell; st, sporogenous tissue; t, tapetum; vn, vegetative nucleus. Scale bar = 33 µm (Figs 1–8), 10 µm (Figs 9, 10).

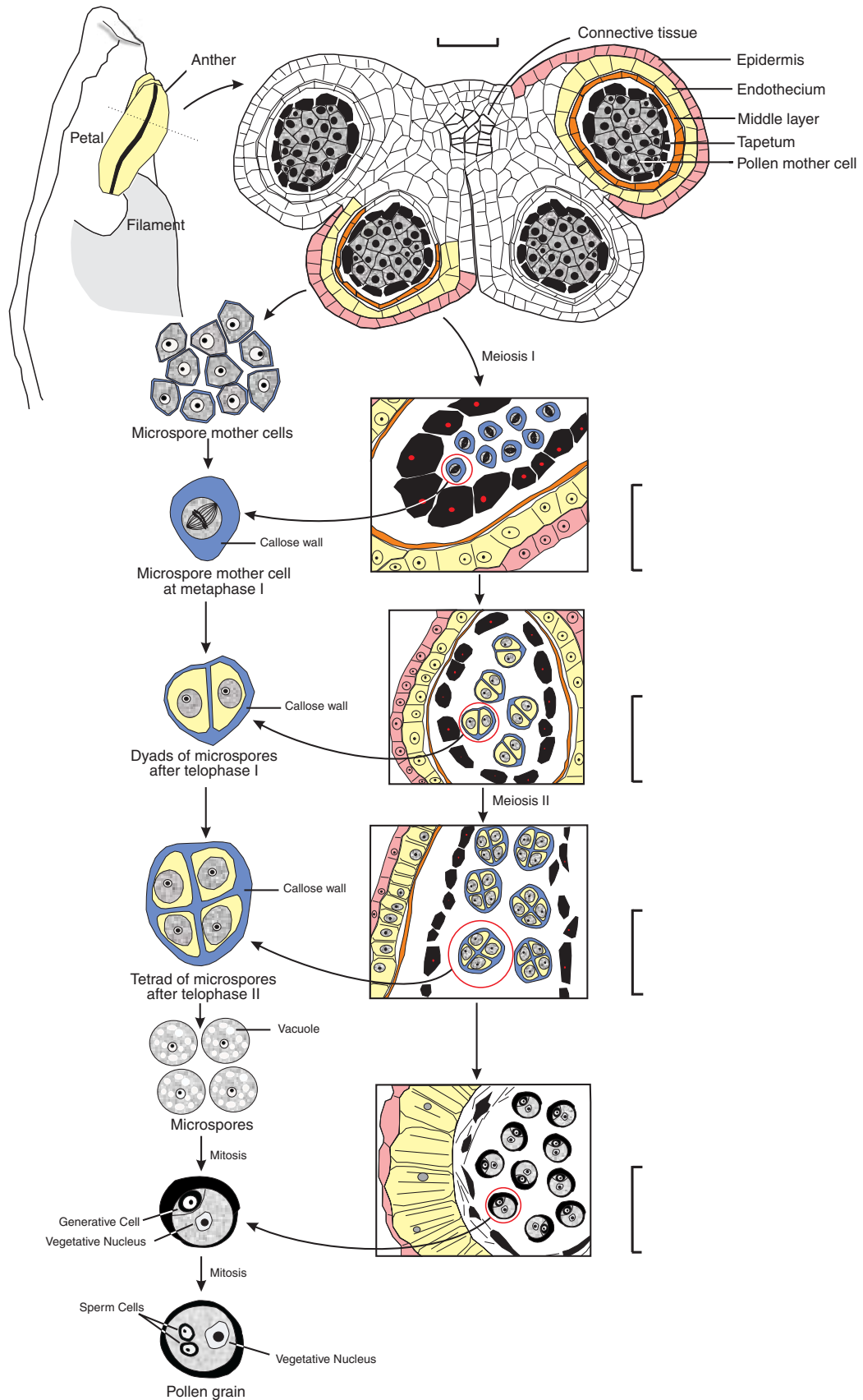


Fig. 11. Diagrammatic representation of pollen development in *Lomandra longifolia*. Scale bars = 33 μ m.

with Sudan IV, for starch with iodine in potassium iodide solution and for protein with Millon's reagent.

To observe and analyse the mature ovules without sectioning, flowers were fixed in FAA (5 parts formalin : 5 parts glacial acetic acid : 90 parts 50% ethanol (v/v/v)) and stored in 70% ethanol. The ovules were dissected out with fine forceps and soaked in Hoyer's fluid (3 g of gum arabic, 20 g of chloral hydrate, 2 mL of glycerol and 5 mL of distilled water as described in Ruzin (1999)) for 24 h at room temperature. The cleared ovules were mounted in Hoyer's fluid and examined by differential interference contrast (DIC) optics on a Nikon Eclipse E800 light microscope and photographed with a mounted Nikon Photo Head V-TP Sensicam camera (PCO CCD imaging).

For scanning electron microscopy (SEM), dehiscing anthers were fixed in 2.5% glutaraldehyde (in 0.1 M potassium phosphate buffer, pH 7.1) at 20°C for 2 h. After thrice rinsing in the same buffer (5 min each), they were dehydrated sequentially in a graded ethanol series (50, 70, 95 and 100%). Samples were critical point dried in CO₂ (BAL-TEC 030 critical point dryer: Bal-Tec, Balzers, Leichtenstein). Pollen grains were dusted on sticky tape affixed to aluminium stubs. Mounted pollens were coated with 20 nm gold palladium in a sputter coater (Edwards E306 A: Edwards Vacuum Systems, Crawley, UK), examined with a Philips 505 SEM (Philips, Eindhoven, Netherlands) operating at an accelerating voltage of 15 KV and photographed with a mounted digital camera.

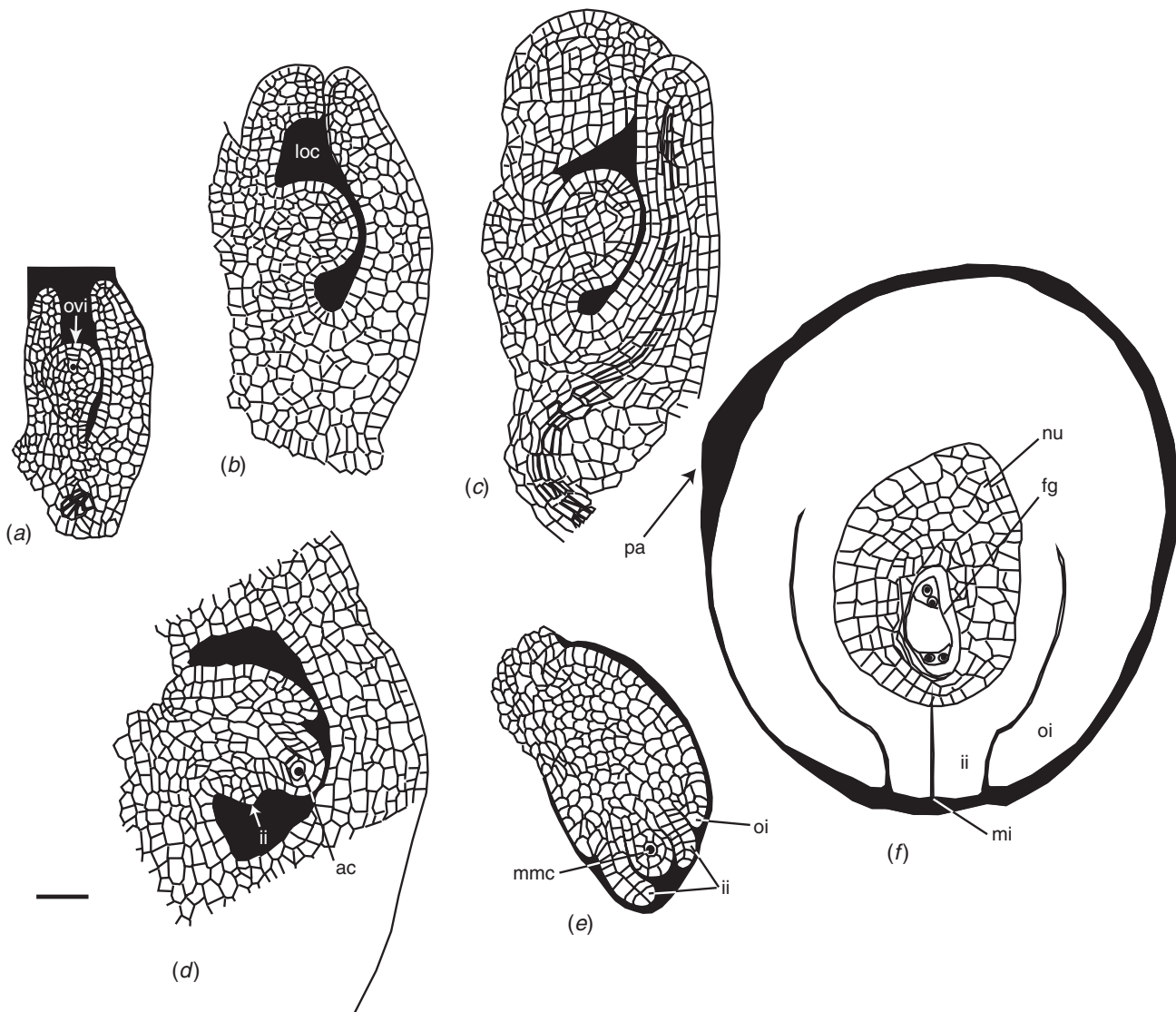
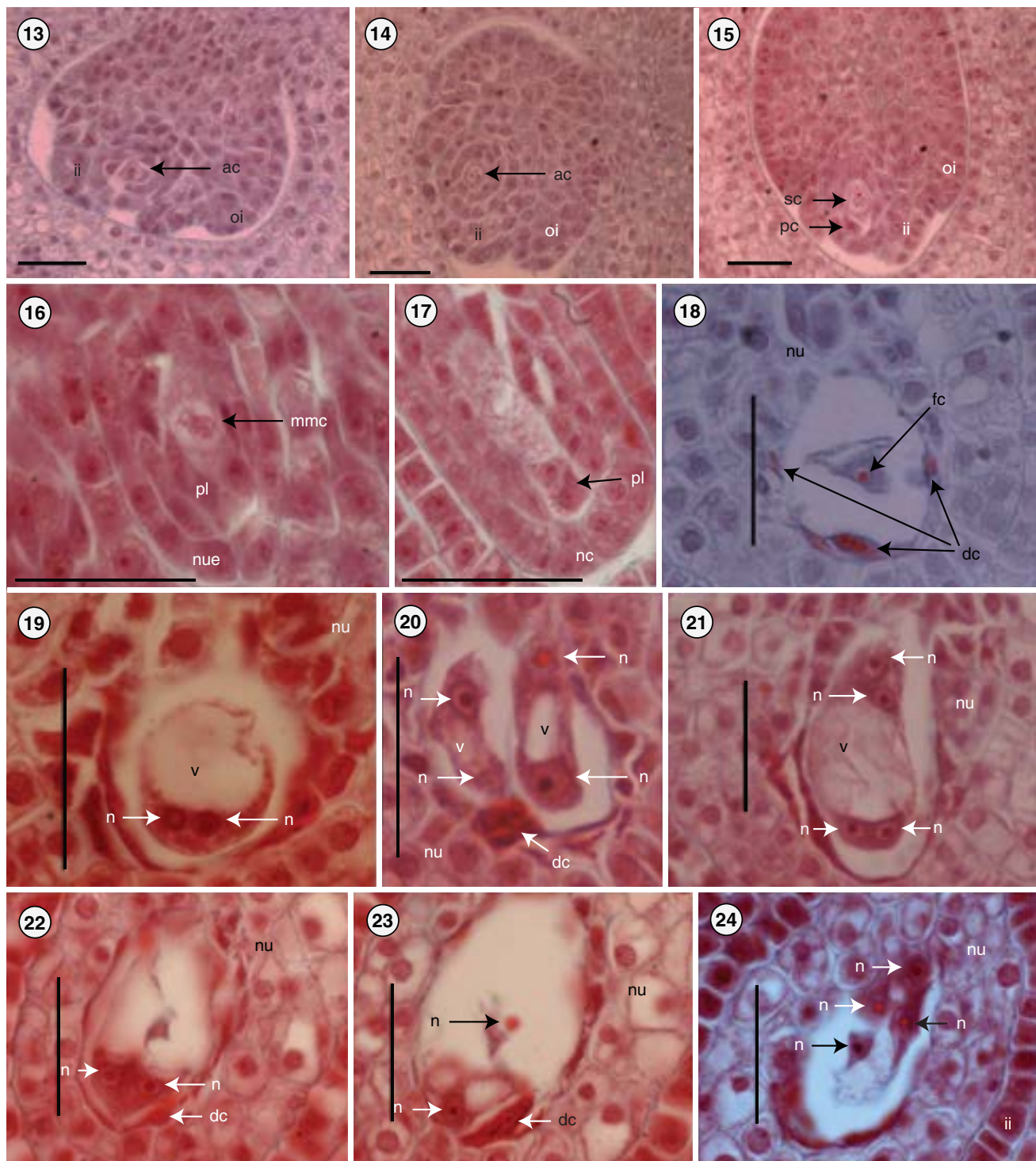
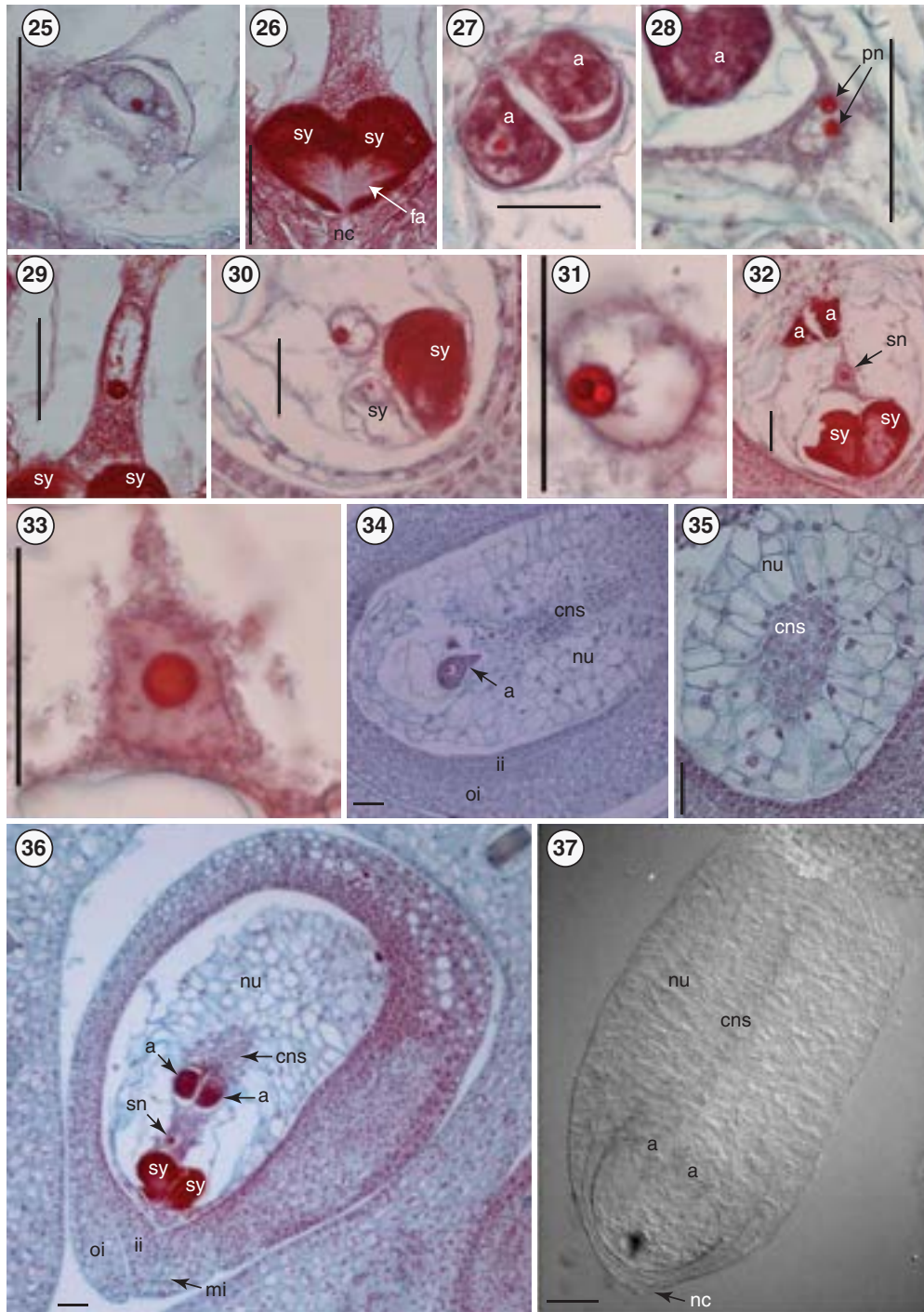


Fig. 12. Ovule and integument initiation in *Lomandra longifolia*. (a) Early erect stage. (b, c) Developing ovule undergoing curvature. (d) Recurving young ovule with enlarged megaspore mother cell in nucellus; inner integument starting to extend over nucellus. (e) Recurving ovule with inner integument just overtopping nucellus and outer integument partially formed. (f) Completely inverted ovule with nucellus overtopped by both integuments; the micropyle is formed by the inner integument which protrudes through the outer integument. The axis of the micropyle forms an angle of ~90° with the plane of attachment of the ovule to the ovary (hemitropous type). ac, archesporial cell; fg, female gametophyte; ii, inner integument; loc, loculus; mi, micropyle; mmc, megaspore mother cell; nu, nucellus; oi, outer integument; ovi, ovule initial; pa, place of attachment. Scale bar = 33 µm.



Figs 13–24. Development of ovule and megasporogenesis in *Lomandra longifolia*. **Fig. 13.** Transverse section (TS) of a young ovule showing the archesporial cell. **Fig. 14.** Longitudinal section (LS) of a young ovule with archesporial cell containing a large nucleus with prominent nucleoli. **Fig. 15.** LS of a young ovule in which the archesporial cell has divided periclinally to form the primary parietal and primary sporogenous cells. **Fig. 16.** LS of a young ovule showing megaspore mother cell at meiotic Prophase I, with two cell layers of parietal tissue separating it from the two-layered nucellar cap. **Fig. 17.** LS of the same specimen showing parietal layer and mode of formation of the nucellar cap by periclinal division in the apical cells of the nucellar epidermis. **Fig. 18.** LS of ovule showing uninucleate embryo sac. **Fig. 19.** Two-nucleate embryo sac (LS). **Figs 20, 21.** Four-nucleate embryo sac (LS). **Figs 22–24.** TS of an ovule at the eight-nucleate stage in different planes of sectioning. ac, archesporial cell; dc, degenerating megaspore; fc, functioning megaspore; ii, inner integument; mmc, megaspore mother cell; n, nucleus in embryo sac; nc, nucellar cap; nue, nucellar epidermis; nu, nucellus; oi, outer integument; pc, parietal cell; pl, parietal layer; sc, sporogenous cell; v, vacuole. Scale bars = 33 μ m.



Figs 25–37. Embryo sac components and mature (8-nucleate) embryo sacs in *Lomandra longifolia*. **Fig. 25.** Egg cell. **Fig. 26.** Synergids. **Fig. 27.** Two of the antipodal cells. **Fig. 28.** Two polar nuclei. **Fig. 29.** Migration of the polar nuclei towards the egg apparatus. **Fig. 30.** Showing two synergids, and two polar nuclei at time of fusion. **Fig. 31.** Magnified view of Fig. 30 showing secondary or fusion nucleus. **Fig. 32.** Showing the two synergids, secondary (fusion) nucleus and two antipodals. **Fig. 33.** Magnified view in Fig. 32 showing secondary or fusion nucleus. **Fig. 34.** Longitudinal section (LS) of a mature ovule showing the embryo sac with one antipodal cell, nucellus (two layers of enlarged dermal cells, subdermal region and central nucellar strand), inner and outer integuments. **Fig. 35.** Transverse section of a mature ovule just above the embryo sac showing the nucellar tissue including the central nucellar strand. **Fig. 36.** Slightly oblique longitudinal section (LS) of a mature ovule showing the embryo sac, nucellus, inner and outer integuments and micropyle. **Fig. 37.** Differential interference contrast view of a cleared mature ovule with the integuments removed, showing three layered nucellar cap directly covering the micropylar end of the embryo sac. a, antipodal cell; cns, central nucellar strand; fa, filiform apparatus; ii, inner integument; mi, micropyle; nc, nucellar cap; nu, nucellus; oi, outer integument; pn, polar nucleus; sn, secondary nucleus (fusion nucleus); sy, synergid. Scale bars = 33 μ m.

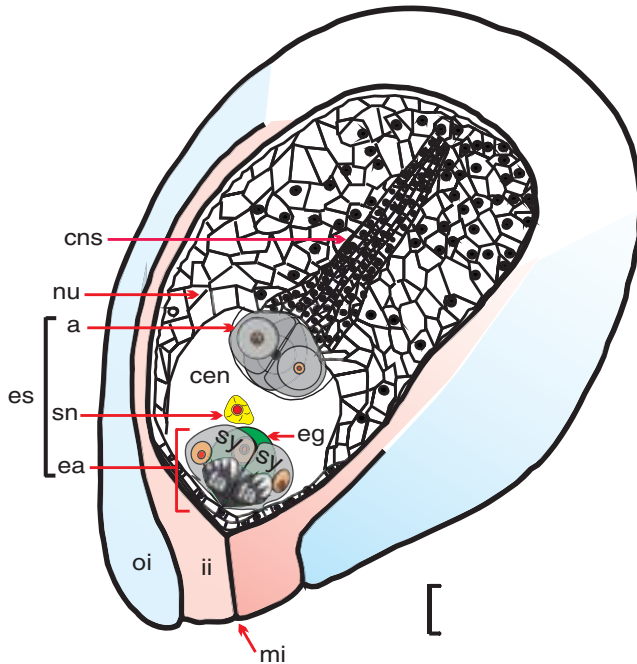


Fig. 38. Longitudinal view of the mature *Lomandra longifolia* ovule reconstructed from light micrographs of 7 μm thick sections. a, antipodals; cen, central cell; cns, central nucellar strand; ea, egg apparatus; eg, egg cell; es, embryo sac; fa, filiform apparatus; ii, inner integument; mi, micropyle; nu, nucellus; oi, outer integument; sn, secondary (fusion) nucleus; sy, synergid. Scale bar = 33 μm .

Results and discussion

Microsporangium

Anthers of *L. longifolia* are tetrasporangiate, with two microsporangia in each lobe (Figs 1, 2). The anther wall before maturity comprises the following four cell layers: an epidermis, an endothecium, one middle layer and a tapetum (Figs 2–5).

The endothecium is a single layer of cells that lies just under the epidermis. During the maturation of the anther, the endothelial cells enlarge and acquire fibrous thickenings.

In cross-section, these cells form a complete ring around each locule. The endothecium becomes irregularly multilayered towards the inner side. This endothecium-like tissue may be contributed by the subepidermal layer of the neighbouring connective tissues which develop fibrous thickening towards the inner side of the anther (Fig. 6). The middle layer is ephemeral and becomes obliterated before the microsporangium is fully mature and ready to dehisce, leaving only a remnant layer against the endothelial wall (Fig. 5).

The anther of *L. longifolia* has one tapetum layer, which is the innermost layer of the anther wall surrounding the sporogenous tissue (Fig. 2). The tapetal cells are uninucleate and remain intact, being of the glandular type (Figs 3, 4).

Microspore mother cells lose contact with the tapetal cells as they enter the phases of meiosis and become enclosed in thick callose walls (Fig. 3).

Meiosis in the microspore mother cell is accompanied by successive cytokinesis. The first meiotic division separates two dyads (Fig. 4); each dyad undergoes Division II, resulting in a tetrad. The cell-plate formation takes place after Meiosis I. The end product of the meiotic divisions is the formation of microspore tetrads with a tetrahedral shape (Fig. 5). Each tetrad is initially enclosed within the mother cell wall which has a gelatinous appearance owing to deposition of callose. The breakdown of this wall liberates individual microspores into the sporangium (Figs 7, 8).

At maturity, the anther epidermis is persistent, the middle layer completely degenerates and the endothecium develops fibrous thickenings in the form of bars that assist the anther to dehisce and release pollen. Thus, the mature anther wall is composed of a persistent epidermis and a fibrous endothecium (Fig. 8). The pollen is shed as single grains (Fig. 9). Developing pollen grains stained deeply with safranin, preventing observation of pollen mitosis. However, staining with acetocarmine allowed identification of a 3-celled pollen (Fig. 10). A diagrammatic representation of all stages of pollen development in *L. longifolia* is presented in Fig. 11.

Ovule morphology

Lomandra longifolia fruit has three loculi and only one ovule per loculus, whereas several ovules per loculus is the most

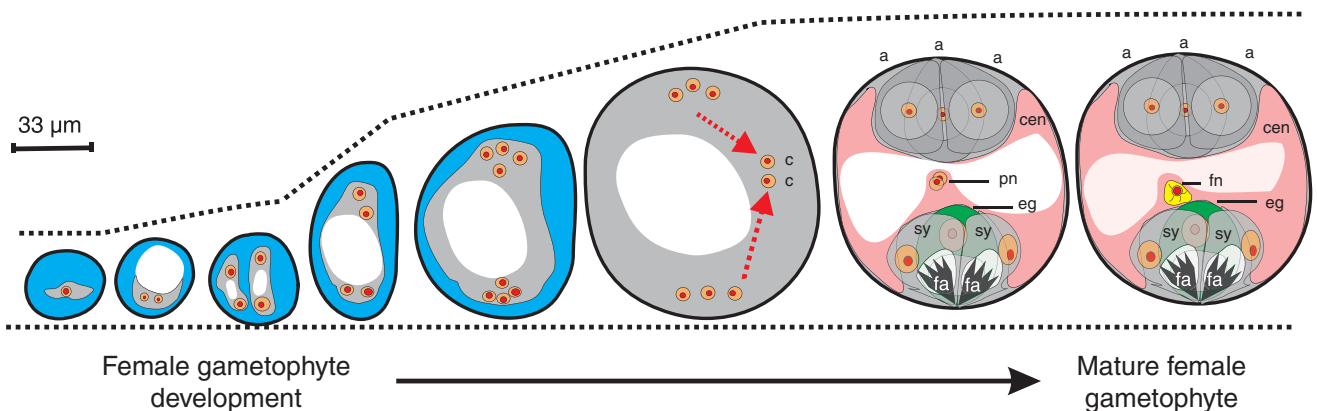
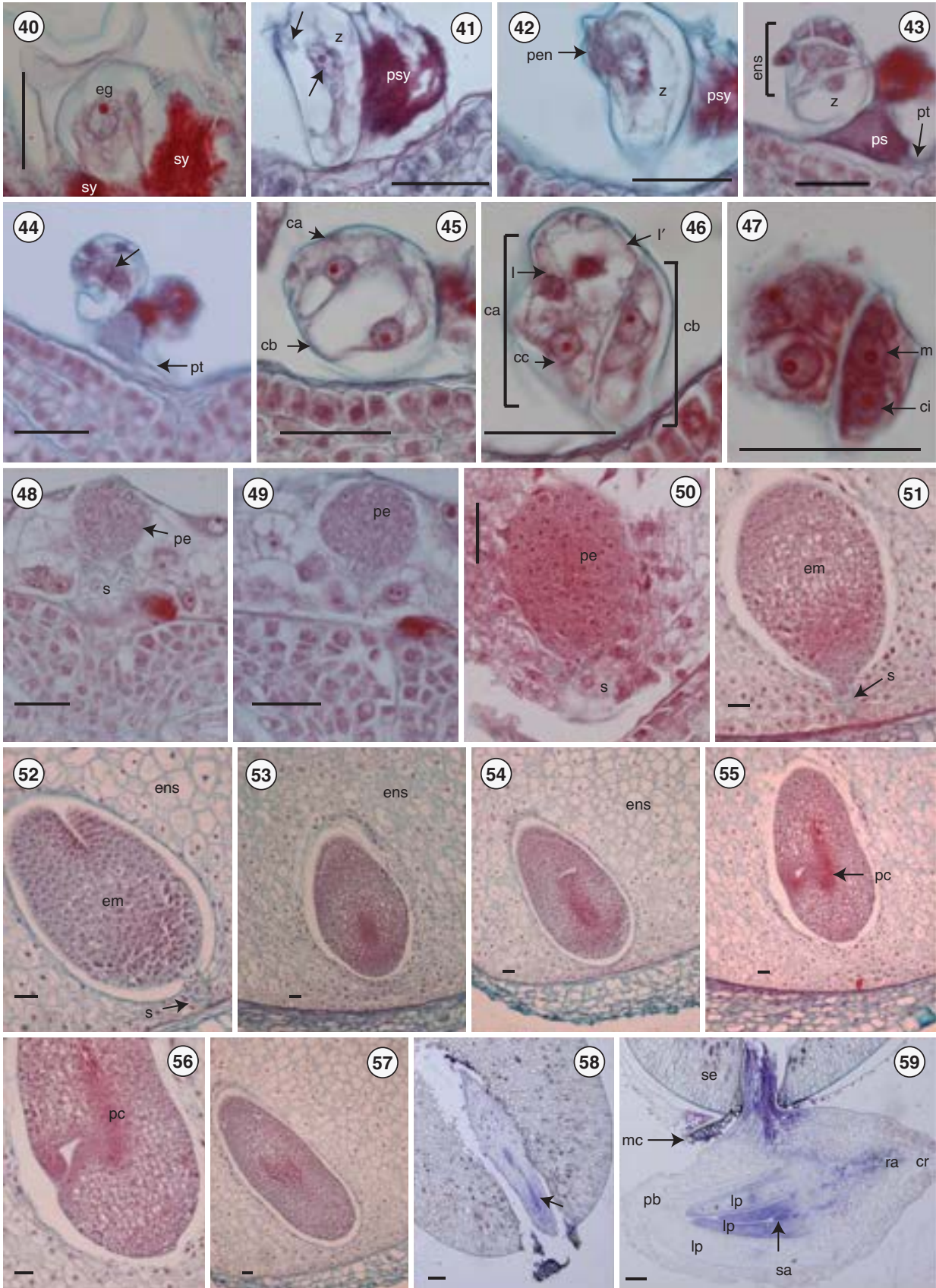


Fig. 39. Reconstructed female gametophyte ontogeny of *Lomandra longifolia*. Chalazal pole is at top and micropylar end at bottom. a, antipodal cell; c, central cell nucleus (or polar nucleus); cen, central cell; eg, egg cell; fa, filiform apparatus; fn, fusion nucleus (secondary nucleus); pn, polar nuclei; sy, synergid cell.



common (and probably the basal) condition in Asparagales. The mature ovule is hemitropous. During its development the ovule undergoes a curvature of 180°, becoming completely inverted, the micropylar axis eventually forming an angle of ~90° with the plane of attachment of the ovule (Figs 12a–f, 80d, e). The ovule is bitegmic, with the micropyle formed by the inner integument (Fig. 12f).

Integuments

The *Lomandra* ovule has two integuments that overgrow the nucellus and arch over its apex. The growth of the integuments is so fast that they enclose the nucellus before fertilisation. The inner integument in *L. longifolia* is initiated before the outer integument (Figs 12d, 13). Histogenetically, the inner integument is formed by cells derived from the dermal layer (dermal origin) and the outer integument by cells derived from both the dermal and subdermal layer (mixed origin) (Figs 12d, e, 13–15).

Micropyle

The micropyle is formed by the inner integument which protrudes through the outer integument (Figs 12f, 36, 38). This is in accord with the situation described in *L. integra* and *L. hastilis* by Rudall (1994) and corresponds closely with the typical Asparagalean type.

Nucellus

The archesporial cell, conspicuous by its larger size, denser cytoplasmic contents and more prominent nucleus (Fig. 13), cuts off a primary parietal cell (Figs 14, 15) which gives rise to two parietal layers (Fig. 16). This is in contrast to the three parietal layers in *L. rigida* shown by Schnarf and Wunderlich (1939; abb. 12, fig. 1, p. 322). The current nucellar classification (Bouman 1984) defines crassinucellate ovules as those in which the megaspore mother cell is separated from the nucellar epidermis by one or more parietal layers; *L. longifolia* is therefore crassinucellate (Fig. 16). The apical cells of the nucellus divide periclinally to form a cap initially two cells thick (Fig. 17) and at maturity three cells in thickness (Figs 36, 37), separating the embryo sac from the micropyle, the parietal layers by this stage having disintegrated. Rudall (1994) found in *L. preissii* that some megasporocytes were one nucellar cell layer from the surface, although most were two, leading her to question the value of this nucellar character in

systematic studies. In *L. longifolia*, we found a consistent pattern of two layers at this stage. Rudall (1994) also reported that in *Lomandra* ovules with mature embryo sacs, the nucellar thickness was usually one cell layer at the micropylar end, which is in marked contrast to the well defined three layers found for *L. longifolia* in our work.

The chalazal region of the nucellus is differentiated into the following three parts: a dermal region with two layers of enlarged cells derived from the nucellar epidermis; a subdermal tissue of irregularly shaped cells; and a strand-like elongated central region consisting of darkly stained small-diameter, axially oriented cells, which did not, however, show any evidence of being pro-vascular (Fig. 34). This type of nucellus has also been observed by Rudall (1994) in *L. integra* and *L. hastilis* as well as in *Thysanotus manglesianus* and *Chamaexeros serra*.

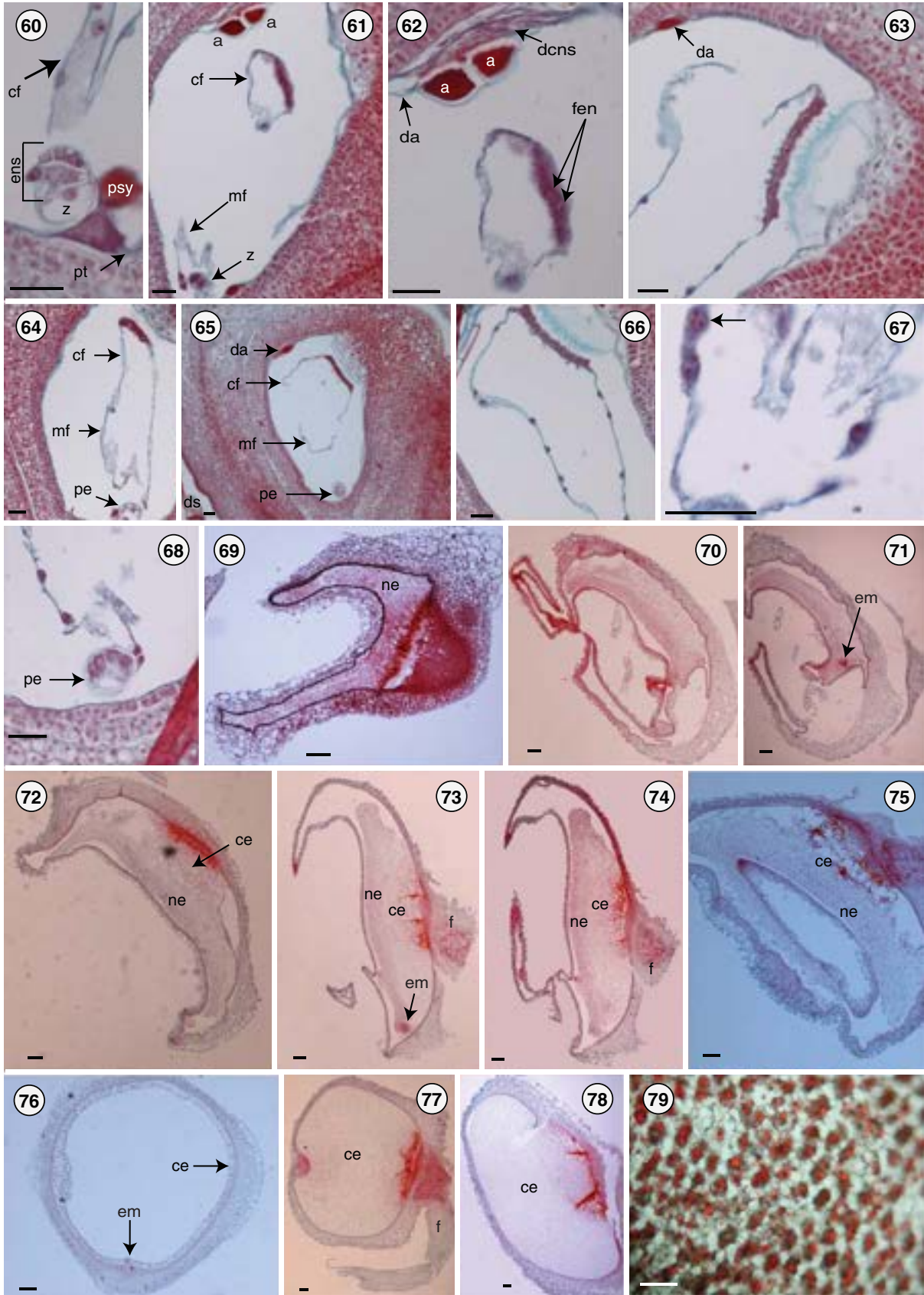
Megasporogenesis

The archesporial cell (Figs 13, 14) divides periclinally to form the primary parietal and primary sporogenous cell (Fig. 15). The primary sporogenous cell does not undergo further mitotic divisions, and functions as the megaspore mother cell (Figs 16, 17). This pattern of archesporial development corresponds to Type III in Schnarf's classification (McLean and Ivimey-Cook 1956, p. 1400). The megaspore mother cell undergoes a linear meiotic division, producing a line of megaspores which were observed in cleared ovules by DIC imaging. One megaspore gives rise to the embryo sac and the remaining three degenerate (Figs 18, 20, 22, 23).

Female gametophyte formation and components of mature embryo sac

Lomandra longifolia has a *Polygonum*-type mature megagametophyte. In the other *Lomandra* species for which information on the mature embryo sac is available (*L. rigida* (Schnarf and Wunderlich 1939); *L. hastilis*, *L. integra*, *L. preissii* and *L. purpurea* (Rudall 1994)), the structure has also been found to be of the *Polygonum* type. The functional megaspore nucleus undergoes three mitotic divisions to form an eight-nucleate megagametophyte containing three enlarged antipodals, an egg apparatus consisting of an egg cell and two very large synergids, and a binucleate central cell (two polar nuclei), altogether occupying a significant part of the embryo sac chamber (Fig. 36).

Figs 40–59. Fertilisation, embryo development and embryo differentiation in *Lomandra longifolia*. The micropylar end is towards the bottom of the page for Figs 40–59. **Fig. 40.** The egg-cell prefertilisation, the lower third obscured by the synergids. **Fig. 41.** The zygote showing what appears to be a sperm nucleus and a cytoplasmic bridge-like structure (arrows). **Figs 42, 43.** Zygote shrinkage. **Fig. 44.** The first asymmetric and oblique zygotic division showing the metaphase plate (arrow), also shown is the pollen tube penetrating one of the synergid cells. **Fig. 45.** Two-celled pro-embryo. **Fig. 46.** Five-celled pro-embryo. **Fig. 47.** The same pro-embryo as in Fig. 46, but in a different plane of sectioning showing the first division (oblique) of the basal cell. **Figs 48–50.** Gradual enlargement and elongation of the pro-embryo through the early globe stage (Fig. 48), later globe stage (Fig. 49) and early elongation stage (Fig. 50) as a result of continued mitotic divisions of the cells derived from the original apical and basal cells. The suspensor is distinct with larger and more vacuolated cells than those in the pro-embryo proper. **Fig. 51.** The embryo before the beginning of differentiation. **Figs 52, 53.** Embryo showing the suspensor (Fig. 52) and the procambial cells (future vascular tissue) at the proximal end of the embryo (Fig. 53). **Figs 54–56.** Elongation and differentiation of the embryo. **Fig. 57.** Cylindrical embryo approaching maturity. **Fig. 58.** A mature embryo showing the vascular tissue (arrow). **Fig. 59.** The whole embryo at the time of seed germination. ca, apical cell; cb, basal cell; cc, cell resulting from the first division of the apical cell; ci, one of the two cells resulting from the first division of the basal cell; cr, coleorrhizae; eg, egg cell; em, embryo; ens, endosperm; I and I', two cells resulting from the third division of the apical cell; lp, leaf primordium; m, one of the two cells resulting from the first division of the basal cell; mc, micropylar cap; pb, protective bract; pc, procambial cells; pe, pro-embryo; pen, primary endosperm nucleus; psy, persistent synergid; pt, pollen tube; ra, root apex; s, suspensor; sa, shoot apex; se, seed; sy, synergid; z, zygote. Scale bars = 33 µm (Figs 38–55), 0.1 mm (Figs 56, 57).



In *L. longifolia*, megagametophyte vacuolation begins at the two-nucleate stage (Fig. 19). At the four-nucleate stage (Fig. 21), the division of the micropylar pair of nuclei gives rise to the synergids (sister cells) and the egg cell and one polar nucleus (sister cells). The division of the chalazal pair gives rise to three antipodals and one polar nucleus. The synergids and antipodals are ephemeral; the egg cell and polar nuclei contribute post fertilisation to the embryo and endosperm, respectively.

The shape and size of the embryo sac changes with time (Figs 18–24, 39). The surrounding nucellus starts to degenerate at the megaspore stage, as the embryo sac enlarges (Fig. 18). The nucellus starts to degenerate uniformly around the functional megaspore cell giving a circular enlargement pattern until the end of the two-nucleate stage (Fig. 19). At the four-nucleate stage, the embryo sac elongates to be twice as long as wide ($\approx 65 \mu\text{m}$ long and $\approx 35 \mu\text{m}$ wide); the micropylar region of the embryo sac at this stage has the same width as the chalazal region ($\approx 25 \mu\text{m}$) but the central region is slightly wider (Fig. 21). Nucellar degeneration continues at a higher rate around the central region of the embryo sac to allow for its expansion, although nucellar-cell degeneration seems to precede megagametophyte expansion (Figs 21–24). Prefertilisation, megagametophytic growth in *L. longifolia* was accommodated by the breakdown of the nucellus and the production of a nucellar lysate rather than by physical disruption, similar to the post-fertilisation megagametophytic growth reported in barley by Norstog (1972) and megagametophyte expansion in maize reported by Russell (1979). The final expansion resulted in the production of a distinctive mature embryo sac which is as broad as it is long ($\approx 100 \mu\text{m}$), spherical in shape and occupying the apex of a long column of nucellar tissue (Figs 34, 36–38). Schnarf and Wunderlich (1939) noted that the mature embryo sac of *L. rigida* was spherical.

The Egg

The egg cell is pear-shaped at the micropylar end and is closely associated with the synergids. It has a distinct vacuole at the micropylar end. Its nucleus, surrounded by cytoplasm, is present at the chalazal end of the cell (Fig. 25).

Only a limited region of the egg cell is in contact with the embryo-sac boundary, most of the cell is surrounded by the synergids and the central cell. The egg cell is highly vacuolated. The portion of the cell distal from the micropyle is almost completely filled with cytoplasm containing the egg nucleus and some small additional vacuoles (Figs 25, 40).

Synergids

The form of the synergids was studied in embryo sacs awaiting fertilisation. The synergids are pyriform and wholly enclosed within the embryo sac; they are enlarged (Fig. 26) and occupy about one-quarter of the length of the embryo sac (Fig. 32). The nucleus, which is more prominent than that in the egg, lies at the chalazal end with a vacuole at the micropylar end (Figs 26, 30). Frequently, the synergids have a lateral hook (Fig. 36) and distinct finger-like infoldings of the wall in the micropylar region, the filiform apparatus (Fig. 26).

One synergid starts to degenerate soon after fertilisation (Figs 41–43) and may play an active role in the nutrition of the embryo sac.

The central cell

The central cell is the largest cell in the embryo sac and is highly vacuolated (Fig. 38). There are two polar nuclei in the central cell located in a thick mass of cytoplasm suspended by cytoplasmic strands in the middle of the cell before fertilisation (Fig. 28); these migrate (Fig. 29) to assume a position in close proximity to the egg apparatus (Figs 30, 31) and subsequently fuse to form the secondary nucleus (Figs 32, 33). Fusion occurs before fertilisation, and after the resulting secondary nucleus is fertilised, it forms the primary endosperm nucleus. The polar nuclei and fusion nucleus are the largest nuclei observed in the embryo sac (Figs 28, 30–33). The central cell contains complex organised cytoplasm which is rich in organelles.

Antipodals and post-fertilisation nucellus

In the undifferentiated 8-nucleate embryo sac, cytokinesis is initiated at the chalazal pole and proceeds in an orderly manner towards the micropyle. The three antipodal nuclei persist as three cells into the post-fertilisation stages (Fig. 27).

The antipodals occupy about one-third of the length of the embryo sac (Fig. 37). Degeneration of the lowest antipodal begins initially, after the cell penetrates deeply into the chalaza, followed by the upper two antipodals (Figs 61–63).

After fertilisation, the central (axial) region of the nucellar tissue remains conspicuous as a mass of smaller and more densely stained cells (Figs 34–36), the antipodals remain prominent (Fig. 36), whereas the surrounding large nucellar cells degenerate in an irregular fashion (Fig. 36). At a slightly later stage (Figs 61, 62), the central nucellar strand becomes degenerate and, with the attached and still intact antipodal cells, takes up a position on one side of the chamber towards the chalazal end (Figs 61–63). The behaviour of the large antipodals is generally in accord with that described by

Figs 60–79. Endosperm formation and development in *Lomandra longifolia*. **Fig. 60.** Early endosperm divisions after double fertilisation. **Figs 61, 62.** Migration of the first portion of the cytoplasmic film with the embedded endosperm nuclei to the chalazal area. **Fig. 63.** Chalazal cytoplasmic film migration with the thickened portion taking up its position in the funicular corner of the chalazal region. **Figs 64, 65.** Fusion of the chalazal and micropylar cytoplasmic films and some free nuclear division. **Fig. 66.** Fused cytoplasmic films forming a ring within the embryo-sac lumen. **Fig. 67.** Fusion of some endosperm nuclei into a polyploid cluster (arrow). **Fig. 68.** Endosperm free nuclei at the five-cell stage of the pro-embryo. **Figs 69–71.** Endosperm development showing free mitotic divisions and the nuclear stage of development. **Figs 72–78.** Cellularisation and the cellular stage of development. **Fig. 79.** Endosperm cells showing oil droplets as food reserve in mature seeds. a, antipodal cell; ce, cellular endosperm; cf, chalazal cytoplasmic film; da, degenerated antipodals; dcns, degenerated central nucellar strand; em, embryo; ens, endosperm; f, funiculus; fen, free endosperm nuclei; mf, micropylar cytoplasmic film; ne, nuclear endosperm; pe, pro-embryo; psy, persistent synergid; pt, pollen tube; z, zygote. Scale bar for = 33 μm (Figs 58–66), 0.1 mm (Figs 67–77).

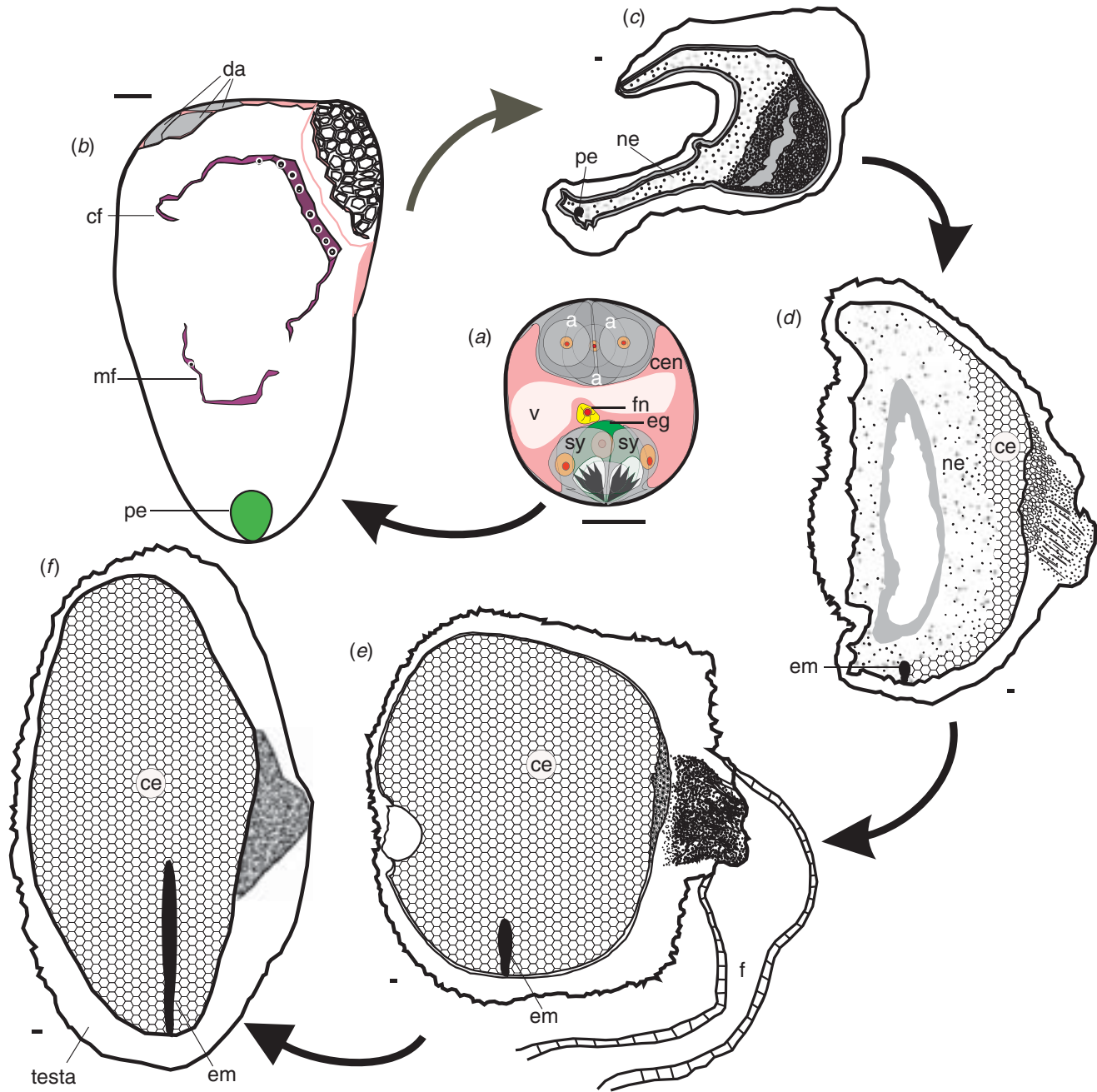


Fig. 80. Summary diagram of the developmental stages of endosperm formation in *Lomandra longifolia*. (a) Embryo sac before fertilisation. (b) Embryo sac after fertilisation showing endosperm formation at the five-cell stage of the pro-embryo. (c) Endosperm formation at the nuclear stage of development. (d) Endosperm development at the beginning of cellularisation. (e) At cellular stage of development. (f) Longitudinal section of a mature seed of *L. longifolia*. a, antipodal cell; ce, cellular endosperm; cen, central cell; cf, chalazal cytoplasmic film; da, degenerated antipodals; eg, egg cell; em, embryo; f, funiculus; fn, fusion nucleus; mf, micropylar cytoplasmic film; ne, nuclear endosperm; pe, pro-embryo; sy, synergid; v, vacuole. Scale bar = 33 μm (a–e), 0.1 mm (f).

Rudall (1994) for the mature megagametophyte of *L. integra* and *L. purpurea*.

Fertilisation and embryogeny

In *L. longifolia*, the pollen tube first comes into contact with the ovule near the funicular end where it begins to grow along the

outer surface of the outer integument towards the micropyle. When the pollen tube reaches the micropylar end of the ovule, it grows through the micropyle (porogamous entry), through the three layers of nucellar cap tissue and into the embryo sac (Fig. 44). The pollen tube then enters into one of the synergids (Figs 43, 44) through the filiform apparatus to release the male gametes, the vegetative nucleus and presumably a limited amount

of tube cytoplasm. The penetrated synergid then undergoes some changes; those resolved by the light microscope included decrease of cellular volume, collapse of the vacuoles and disintegration of the plasma membrane (Fig. 41). The low transparency of the penetrated synergid in optical microscopy (owing to the dense staining properties of the synergids' cytoplasm) limited the observations and interpretations of the stained sections.

Tracing the actual transfer of the sperm cells from the penetrated synergid to and into the egg cell and the central cell respectively, was not possible. However, what appears to be a sperm nucleus was identified in the egg cell shortly after fertilisation and a cytoplasmic bridge-like structure was observed between the egg cell and the penetrated synergid cell (Fig. 41). If confirmed by further work, this observation would support the hypothesis proposed by Linskens (1968), van Went (1970) and Jensen (1972), who each stated that fertilisation in angiospermous plants includes a true cell-fusion process, which leads to the formation of cytoplasmic bridges between the gametes through which the sperm nucleus and possibly the sperm cytoplasm can pass. Remnants of the male-gamete cytoplasm, identified in other studies as x-bodies (Jensen and Fisher 1968), could not be seen in the penetrated synergid because of its low transparency; however, some partly visualised darkly stained bodies were suspected to be degenerated synergid nuclei. Directly after cell fusion some sections clearly showed an increase in density of unidentified cytoplasmic organelles inside the egg cell and the central cell (Figs 26, 41).

Zygote

The zygotic cell was polarised distinctly, with the micropylar pole being vacuolated, whereas the chalazal pole contained the nucleus and most of its cytoplasm (Figs 42, 43), thereby keeping the same polarity as the unfertilised egg cell.

Following suspected intense metabolic activity shortly after fertilisation, the young zygote showed a cluster of cytoplasmic organelles around the apically located nucleus, owing possibly to internal differentiation and/or multiplication of the organelles present in the original egg cytoplasm (Fig. 41). The fertilised egg in *L. longifolia* undergoes a dramatic decrease in size before embarking on division. The volume of the zygote decreases to about half the size of the egg before fertilisation (Figs 41–43). Similarly, in taxa such as *Gossypium* and *Hibiscus* the volume of the zygote decreases (Pollock and Jensen 1964; Jensen 1968; Ashley 1972). In contrast, *Cypripedium* (Poddubnaya-Arnoldi 1967), *Jasione* (Erdelska 1997) and *Arabis* (Czapik 1974) show enlargement of the zygote. Possible explanations of such different behaviours were given by Czapik and Izmailow (2001).

Early embryogenesis

The first zygotic division in *L. longifolia* does not occur immediately after fertilisation, the zygote remaining quiescent for a period of time. In most embryogeny types, the first division is transverse and asymmetrical, in accordance with the asymmetrical position of the nucleus (Natesh and Rau 1984). However, the first mitotic division of the zygote in *L. longifolia*

was oblique and asymmetric (Fig. 44), giving rise to a larger and vacuolated basal (micropylar) cell (*cb*) and a smaller apical (chalazal) cell (*ca*) (Fig. 45). The next division is the first division of the basal cell, the new wall being asymmetric and making an oblique angle with the wall from the previous division, to produce cells *ci* and *m* as shown in Fig. 47. This is followed by the first division of the apical cell (*ca*) to produce the daughter cells *cc* and *cd*, after which *cd* divides to form cells *l* and *l'* (Fig. 46). These three apical cells, together with the two basal cells, form a five-celled pro-embryo. This characteristic and the distinct pattern of pro-embryonic development conforms to the Graminad type as defined by Batygina (1969) and recognised as a standard type by Czapik and Izmailow (2001).

Differentiation of the embryo

After the zygote divides, both the apical and basal cells contribute to the production of the pro-embryo. This develops in a pocket within the endosperm, and in the early stages, the proximal end is physically connected to the endosperm by a short suspensor. The pro-embryo grows and changes in shape from a globular structure (Figs 48–50) to a cylindrical embryo (Figs 51–57) in which the various embryonic structures including the cotyledon, coleoptile primordium, shoot apex and root apex are progressively differentiated.

Table 1. A summary of embryological features of *Lomandra longifolia*

Character	Description
Anther and microspores	
Number of sporangia	Four
Anther wall development	Monocotyledonous type
Tapetum	Glandular
Nucleation of tapetal cells	Uninucleate
Cytokinesis in meiosis	Successive
Shape of microspore tetrad	Tetrahedral
Anther epidermis at maturity	Persistent
Endothecium at maturity	Fibrous
Middle layer at maturity	Obliterated
Ovule, nucellus and megagametophyte	
Ovule orientation	Hemitropous
Nature of nucellus	Crassinucellate
Archesporium	Single celled
Archesporial development pattern	Schnarf's type III
Number of parietal cell layers	Two
Shape of megaspore tetrad	Linear
Mode of embryo sac formation	<i>Polygonum</i> type
Antipodal cells	Ephemeral
Number of integuments	Two
Thickness of inner integument	Two cell layers
Thickness of outer integument	Four cell layers
Micropyle formation	By inner integument
Histological origin of inner integument	Dermal
Histological origin of outer integument	Dermal and subdermal
Thickness of mature nucellar cap	Three cell layers
Mode of pollen tube entry to ovule	Porogamous
Mode of endosperm formation	Nuclear type
Endosperm food reserve	Mostly oil
Mode of embryogenesis	Graminad type
Suspensor	Short, wide

Endosperm formation and development

The endosperm, a product of double fertilisation, develops only in angiosperms. A male gamete fuses with the polar nuclei, or the secondary nucleus in the case of *L. longifolia*, to produce the primary endosperm nucleus. The division of the primary endosperm nucleus and repeated divisions of the daughter nuclei lead to the formation of the endosperm tissue.

The primary endosperm nucleus and the daughter nuclei undergo free-nuclear divisions. At this stage, the endosperm was seen as several nuclei joined by cytoplasm; these nuclei remain embedded in a cytoplasmic sheath in the micropylar region (Fig. 60). The first partition of the cytoplasmic sheath produces a film of cytoplasm which is very thick in the middle and thin at both ends (Figs 61, 62). This cytoplasmic film, which has 12–15 free nuclei still distributed within, migrates to the chalazal region so that the thick part of the film becomes located slightly above the place of attachment of the ovule and is now referred to as the chalazal cytoplasmic film (Fig. 63). The second partition of the cytoplasmic sheath produces the micropylar cytoplasmic film (Fig. 61) which is shorter than the first one and has fewer nuclei (5–8 nuclei) within it. This second film, which is thin and lacks a heavily stained region, migrates a short distance from the micropylar region and connects with the first cytoplasmic film to form a ring (as seen in longitudinal sections) within the embryo-sac lumen (Figs 64–66). At times, some of the nuclei may fuse to form polyploid clusters (Fig. 67). This pattern of endosperm development is known as the nuclear type. In this connection it is interesting to note that Schnarf and Wunderlich (1939, p. 322) concluded their discussion of the embryo sac of *L. rigida* by saying that because of its limited size they were unable to suggest whether the pattern of endosperm development would be helobial or not. The answer, at least for *L. longifolia*, is a definite no.

Embryo development seems to begin when both cytoplasmic films are established (Figs 64, 65). Wall formation (cellularisation) in the endosperm is initiated around the placental region and gradually extends towards the opposite side (Figs 72–75). Wall formation continues until there are no remaining free nuclei. The cells become filled with reserve food (largely oil (Fig. 79), some protein but no starch) as the seed matures (Figs 76–79). A diagrammatic representation of all stages of endosperm development in *L. longifolia* is shown in Fig. 80. Embryological features of *L. longifolia* are summarised in Table 1.

Conclusions

This detailed study of the embryology of *L. longifolia* provides a firm basis for future comparative studies within the genus *Lomandra* and closely related genera.

Our findings in relation to the mature embryo sac are in broad agreement with those reported by Schnarf and Wunderlich (1939) and Rudall (1994). However, on one point there is a considerable difference which may be of some importance. Rudall (1994), working from information gathered from her own studies of the mature embryo sac of four species of *Lomandra* and a brief published account of one other species, stated that '*Lomandra* has a very distinctive mature megagametophyte, with giant synergids and antipodal cells, almost completely filling the chamber'. Our

studies of *L. longifolia* indicate that this generalisation will have to be modified because the synergids and antipodals of this species, although large (Figs 36, 37), could by no means be described as 'almost completely filling the chamber'. Lee and Macfarlane (1986), following generally the earlier subgeneric classification of Bentham (1878), divided *Lomandra* into four sections and the largest section into two series. To what extent the proportion of the embryo sac, which is occupied by the synergids and antipodals, has any systematic significance within the genus *Lomandra* remains a subject for future study. It is worth noting, however, that none of the *Lomandra* species for which original observations are reported by Rudall belongs to the same group as *L. longifolia*, whereas *L. rigida*, as depicted by Schnarf and Wunderlich (1939), has much less bulky synergids and antipodals and belongs to the same subgeneric section and series as *L. longifolia*.

The zygotic and early pro-embryonic divisions in *L. longifolia* are distinctly oblique rather than transverse. These early divisions conform geometrically to the Graminad type of embryogenesis as defined by Batygina (1969). This would appear to be the first report of the occurrence of the Graminad pattern outside the grass family (Poaceae). Finally, the details of endosperm formation and development present several unusual features that deserve future comparative studies with other species within the Lomandraceae and related families.

Acknowledgements

We express our deep gratitude to Dr Jane Radford, manager of the Histopathology Laboratory at the University of Sydney, for permission to work in her laboratory and for her help on numerous practical matters. Thanks are also due to Professor R. A. McIntosh and Miss Alexandra Freebairn for assistance in the preparation of the manuscript. Finally we thank Leppington Speedy® Seedlings Pty Ltd for the provision of plant material and financial support.

References

- APG (1998) An ordinal classification for the families of flowering plants. *Annals of the Missouri Botanical Garden* **85**, 531–553. doi: 10.2307/2992015
- APGII (2003) An update of the Angiosperm Phylogeny Group classification for the orders and families of flowering plants: APG II. *Botanical Journal of the Linnean Society* **141**, 399–436. doi: 10.1046/j.1095-8339.2003.t01-1-00158.x
- Ashley T (1972) Zygote shrinkage and subsequent development in some *Hibiscus* hybrids. *Planta* **108**, 303–317. doi: 10.1007/BF00389308
- Australian Plant Name Index (2008) IBIS database, Centre for Plant Biodiversity Research, Australian Government, Canberra. <http://www.cpbr.gov.au/cgi-bin/apni> [verified 22 August 2008].
- Batygina TB (1969) On the possibility of a new type of embryogenesis in angiosperms. *Revue de Cytologie et de Biologie Vegetales* **32**, 335–341.
- Bedford DJ, Lee AT, MacFarlane TD, Henderson RF, George AS (1986) Xanthorrhoeaceae. *Flora of Australia* **46**, 88–171.
- Bentham G (1878) 'Flora Australiensis: a description of the plants of the Australian Territory. Vol. VII.' (L. Reeve & Co.: London)
- Bentham G, Hooker JD (1880) 'Genera Plantarum. Vol III.' (Lovell Reeve & Co.: London)
- Bouman F (1984) The ovule. In 'Embryology of angiosperms'. (Ed. BM Johri) pp. 123–157. (Springer-Verlag: Berlin)

- Brummitt RK (1992) 'Vascular plant families and genera.' (Royal Botanic Gardens, Kew: London)
- Cronquist A (1981) 'An integrated system of classification of flowering plants.' (Columbia University Press: New York)
- Czapik R (1974) Embryology of five species of the *Arabidopsis hirsuta* complex. *Acta Biologica Cracoviensia. Series: Botanica* **27**, 13–25.
- Czapik R, Izmailov R (2001) Zygotic embryogenesis, structural aspects. In 'Current trends in the embryology of angiosperms'. (Eds SS Bhojwani, WY Soh) pp. 197–222. (Kluwer Academic Publishers: Dordrecht, The Netherlands)
- Dahlgren RM, Clifford HT, Yeo PF (1985) 'The families of the monocotyledons.' (Springer-Verlag: Berlin)
- Davis GL (1966) 'Systematic embryology of the angiosperms.' (John Wiley & Sons: New York)
- Erdelska O (1997) Structural aspects of fertilization and embryogenesis in angiosperms. *Acta Universitatis Carolinae Biologica* **41**, 49–66.
- Jensen WA (1968) Cotton embryogenesis. The zygote. *Planta* **79**, 346–366. doi: 10.1007/BF00386917
- Jensen WA (1972) 'The embryo sac and fertilization in angiosperms. Harold L Lyon Arboretum Lecture Number Three.' (University of Hawaii: Honolulu)
- Jensen WA, Fisher DB (1968) Cotton embryogenesis: the entrance and discharge of the pollen tube in the embryo sac. *Planta* **78**, 158–193. doi: 10.1007/BF00406648
- Krause K (1930) Liliaceae. In 'Die Natürlichen Pflanzenfamilien'. 2nd edn. 15a. (Eds A Engler, K Prantl) pp. 227–386 (Engelmann: Leipzig, Germany)
- Lee AL, Macfarlane TD (1986) *Lomandra*. *Flora of Australia* **46**, 100–141.
- Linskens HF (1968) Egg-sperm interaction in higher plants. *Accademia Nazionale dei Lincei* **104**, 47–60.
- McLean RC, Ivimey-Cook RW (1956) 'Textbook of theoretical botany. Vol. II.' (Longmans, Green & Co: London)
- Natesh S, Rau MA (1984) The embryo. In 'Embryology of angiosperms'. (Ed. BM Johri) (Springer-Verlag: Berlin)
- Norstog K (1972) Early development of the barley embryo: fine structure. *American Journal of Botany* **59**, 123–132. doi: 10.2307/2441390
- Poddubnaya-Arnoldi VA (1967) Comparative embryology of the Orchidaceae. *Phytomorphology* **17**, 312–320.
- Pollock EG, Jensen WA (1964) Cell development during early embryogenesis in *Capsella* and *Gossypium*. *American Journal of Botany* **51**, 915–921. doi: 10.2307/2440240
- Rudall P (1994) The ovule and embryo sac in Xanthorrhoeaceae *sensu lato*. *Flora* **189**, 335–351.
- Rudall P, Chase MW (1996) Systematics of Xanthorrhoeaceae *sensu lato*: evidence for polyphyly. *Telopea* **6**, 629–647.
- Russell SD (1979) Fine structure of megagametophyte development in *Zea mays*. *Canadian Journal of Botany* **57**, 1093–1110. doi: 10.1139/b79-134
- Ruzin SE (1999) 'Plant microtechnique and microscopy.' (Oxford University Press: New York)
- Sass JE (1958) 'Botanical microtechnique.' 3rd edn. (The Iowa State University Press: Ames, IO)
- Schnarf K, Wunderlich R (1939) Zur vergleichenden Embryologie der Liliaceae–Asphodeloideae. *Flora* **133**, 297–327.
- van Went JL (1970) The ultrastructure of the fertilized embryo sac of *Petunia*. *Acta Botanica Neerlandica* **19**, 468–480.

Manuscript received 17 December 2007, accepted 30 October 2008